IOSR Journal of Applied Geology and Geophysics (IOSR-JAGG)
e-ISSN: 2321–0990, p-ISSN: 2321–0982.Volume 8, Issue 1 Ser. II (Jan – Feb 2020), PP 23-35
www.iosrjournals.org

Employing the geophysical and hydrological data for the evaluation of the groundwater occurrences in Baharyia Oasis, Egypt

Alhussein Adham[1]
[1](*Geology Department, Faculty of Science, Helwan University, 11790 Ain Helwan, Cairo, Egypt.)*

Abstract:
Bahariya oasis is a great syncline in the Egyptian Western Desert. Because of the overpopulation in Bahariya oasis in the past 40 years, it is important to extract as much groundwater as possible to expand the agricultural lands and fulfill people's needs of water and crops. Being far away from the River Nile, it is very essential to investigate the groundwater existence and its origin on it. The present study utilizes vertical electrical soundings (VES'es) and time domain electromagnetic soundings (TDEM) to study the investigated area. The main objective of this study is to give a detailed description of the main subsurface conditions of groundwater existence, hydrochemistry, potentiality, and its depth and quality. Geophysical analysis and interpretation of the obtained findings expose that the subsurface is composed of five geoelectrical layers with a clear general slope from southwest towards the northeast. The fourth and the fifth layers are considered the two water bearing formations; whereas the fourth layer is saturated with the fresh water that lies above the fifth brackish water layer. By analyzing the samples of groundwater, it is found that they are geochemically homogenous. The groundwater genesis belongs to Nubian sandstone aquifers system and mainly Na-Ca-SO4-Cl type. The findings demonstrate that the study area has high potentialities of groundwater in two main Nubian Sandstone aquifers: shallow fresh water and deep brackish water. The lithological and structural components have mainly no supply in recharging and depending on pluvial waters storing. The geochemical characteristics of the groundwater of the examined aquifers reveal meteoric water, which is a fresh to slightly brackish water. The moderately groundwater salinity happens by silicate evaporation and weathering processes taking place in the Cenomanian aquifers matrix. Furthermore, a good number of the samples of the examined groundwater are unsuitable for human use. These samples are too adequate to poultry and livestock. In addition, the used hydrogeological monitoring to this area shows high groundwater potentialities that will help in the upcoming development.
Key Word*: Vertical electrical Sounding (VES), Time Domain Electromagnetic Sounding (TDEM), hydrochemistry, Bahariya Oasis area, Egypt.*

Date of Submission: 13-01-2020 Date of acceptance: 29-01-2020

I. Introduction

Baharyia oasis is one of the well-known six large oases in the Western Desert. It is about 370 km far from Cairo, the capital of Egypt. The investigated region is located between latitudes 27° 42' 52.39" and 28° 33' 29" N, and longitudes 28° 25' 37.53" and 29° 16' 49.38" E, and covers a siteabout2500 km² (Fig.1a). The present study investigates the subsurface water content of Baharyia oases that are interpreted from geophysics and geochemistry. Regionally, the investigated area includes three central topographic types involving hilly areas, Syncline floor and Plateau surface (Fig. 1b) [1]. The hilly areas are formed of Upper Cretaceous rocks. They are scattered within the syncline floor and have dissimilar shapes varying between conical shapes to flat tops. The syncline floor, which is oval shaped, consists of Lower Eocene rocks [2]. The Plateau surface, which mostly consists of Lower Eocene carbonates, surrounds the Oasis and its scarp which is found by the Upper Cretaceous rocks [3]; [4];[5].

It is expected that the estimated drawdown of the El-Bahariya Oasis varies from 3 to 26 m with minimum water distribution over the upcoming 25 years [6].

Many researchers are interested in this area, but they have either carried out studies on parts of it or studied it in different ways, including geology, hydrology, well logging, and geophysics [7]; [8]; [9]; [10]; [11]; [12]; [6]; [13];[14].

Attraction researches are widely utilized as part of surveys of groundwater in which the structural detection was the key objective (i.e., [15]; [16]; [17]; [18]). For the purpose of investigating the groundwater, the electrical resistivity and electromagnetic tools, which utilize the VES and TEM techniques, are widely employed owing to the high conductivity or low resistivity of groundwater but in separated parts of the oasis

(i.e., [19]; [20]; [21]; [22]; [23]; [24]). Numerous groundwater studies are conducted in the Egyptian western desert.

This research is distinctive in defining the impact of groundwater aquifers and its geochemistry on in Baharyia oasis by using hydrological and geophysical tools. This helps in redrawing the groundwater aquifer maps of Baharyia oasis.

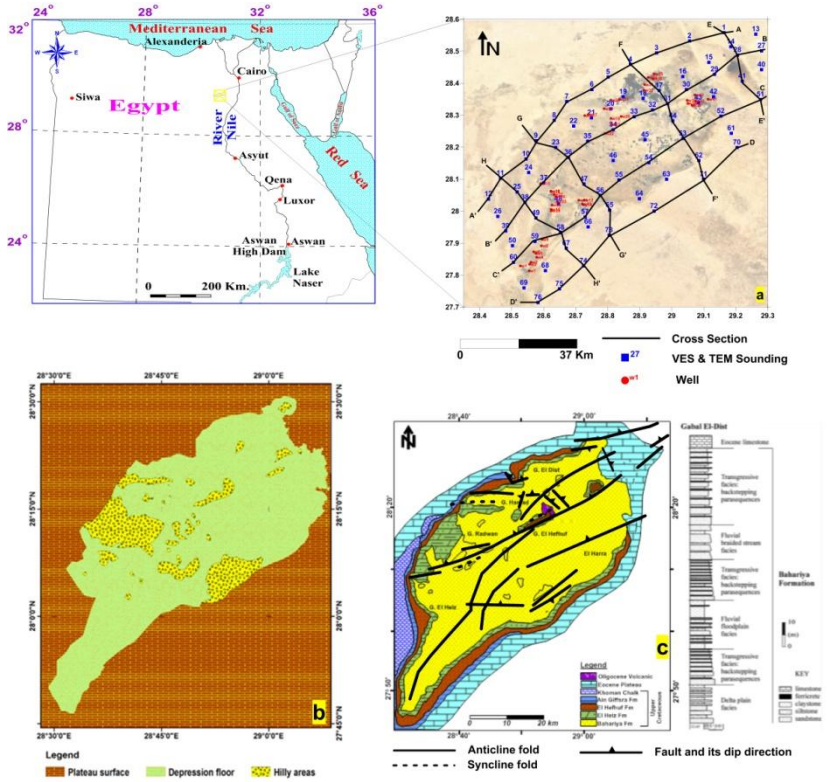

Figure No. 1. a) The location map of the investigated region, b) Topographic types map, c) Geology map of the investigated region showing the places of the old detected structures (after [3]).

II. GEOLOGY

Bahariya oasis, which is part of a large Syrian Arc belt in north western Desert ([25]; [26]; [27]), is an eroded anticline (length 115 km; width 45 km). This anticline is created through an extensional tectonic followed by contraction tectonic. The extension phase coincided with the opening of the Neo-Tethys in Triassic, while the first contraction matched with closing the Neo-Thetys and the merging of the Eurasian plate together with the African-Arabian plate in Late Cretaceous [28].

Along El Bahariya Oasis, several lithological units range between Upper Cretaceous and Oligocen [29]. The Nubian rocks signify the oldest uncovered sedimentary rocks [29]; [30]; [31]; [32]; [33]; [34]; [35]; [36]; [37]; [38]. Bahariya Formation (Early Cenomanian) forms floor and the isolated hills in the Oasis. It consists of +170 m thick fluviatile sequences of sandstone and siltstone. El Heiz Formation (Late Cenomanian) overlies Bahariya Formation at the scarp base. It is composed of ~ 30 m thick alternating sandstone and shale with interbreded carbonate. El Hefhuf Formation (Campanian) crops out in the eastern and western edges of the oasis and in some of the isolated hills. It basically consists of dolostone and sandstone with sandy clay intercalations. Khoman Chalk (Maastrichtian) has 25 m thick and it consists of white massive chalk and chalky limestone beds. The Middle Eocene is well exposed in the plateau and distinguished into Naqb, Qazzun and Hamra Formation. They are made of white limestone, dolomitic limestone and chalky limestone rocks. The Oligocene in the Bahariya is symbolized by extrusive basalt.

III. Material And Methods

Vertical Electrical Sounding and Profiling

Vertical Electrical Sounding (VES) is the best helpful technique for groundwater investigation. All types of resistivity measurements attempt to identify the change in the resistivity values in a vertical and horizontal way. So as to attain one the basic goals of such a study, seventy six (76) VES stations are measured to define the geoelectrical layers in the investigated region area, water bearing layers and the structures influencing these layers. Direct current resistivity meter [39] is used to accumulate data-related field by utilizing Schlumberger separation with current electrodes configuration whose length is 2000m. Near to the drilled wells,

certain VES stations have been measured so as to compare the geoelectrical measurements with layers' thickness, water-bearing layers' depth and lithology's succession [40]. So as to achieve the interpretation related to the field data, the existing geological, hydrological and well information are utilized and modeled. [41] and [42] software are used to attain the final model. Because of the interpretation data, a map is drawn to select the preeminent location to drill new prolific wells and redraw the groundwater map of the investigated region.

Schlumberger configuration is utilized to measure seventy six (76) profiling stations to investigate horizontal variants in the values of apparent resistivity at various depths and to identify the local structures in the investigated region (Fig. 1a). The distribution of VES stations tries to cover the whole location of the investigated region. The interpreted data are employed to draw clear maps to clarify the horizontal changes in the apparent resistivity values at different depths.

Time-domain Electromagnetic Sounding and Profiling

The TEM survey utilizes [43] instrument in this research. The instrument detects the conducting materials of underground through transmitting electrical pulses along cupper cable placed on the ground. This instrument is distinctive because it has both receiver and transmitter in the same unit. In this study, the used cupper cable loop has diameters100m x100m squares with a very short period of time as 0.23-0.37 milli.sec.

The seventy six (76) TEM sounding stations (Fig. 1a) are measured in the similar locations of VES stations to support the interpreted data of the two surveys to approximately reach the final lithological and Geoelectrical model [44]. ZONDTEM1D [45] software has been utilized in the electromagnetic sounding interpretation.

Hydrochemistry

The hydrochemical characterization of the groundwater samples at Bahariya Oasis is evaluated using major ions; K^+, Na^+, Mg^{++}, Ca^{++}, Cl^-, $SO4^{-2}$ and HCO^{3-}.The chemical analysis data of 42 water samples (Table 1) are plotted on [46], [47], and [48] diagrams using [49]Software to identify water types and origin.

[48] diagram is a composite plot consisting of two ternary diagrams where the milliequivalents percentages (e %) of the cations are plotted against that of anions. The data points in the two base ternary diagrams are interpolated into square (combined field of Na^{++}, K^+ and $HCO3^-$) of the main field which lies perpendicular to the third axis in each triangle [50]. It shows the clustering of water quality and displays some possible geochemical processes that may affect the water genesis [51].

[47] diagram provides a convenient way to present chemical composition of groundwater.

[46] diagram is a multifaceted plot wherein milliequivalents percentage (e%) concentrations of major ions; K^+, Na^+, Mg^{++}, Ca^{++}, Cl^-, $SO4^{-2}$ and $HCO3^-$ are plotted in two triangular fields, which are then projected further into the central diamond field.

Relations between major cations and anions are determined using Pearson's correlation (Table 2). A high correlation coefficient (near 1 or -1) means a good relationship between two variables and its value around zero means no relationship. More precisely parameters, which show that $r > 0.5$, are considered to be strongly correlated [52]. The matrix (Table 2) shows strong positive correlation of TDS with Na^+, Cl^-, Mg^{+2}, Ca^{+2} and K^+ (0.9, 0.88, 0.87, 0.797 & 0.75, respectively).

Table 1. Hydrochemical analyses of the collected groundwater samples, Bahariya Oasis, Western Desert, Egypt

Sample No.	EC (µmohs/cm)	TDS (ppm)	pH	CATIONS				ANIONS		
				K^+	Na^+	Mg^{++}	Ca^{++}	Cl^-	SO_4^{--}	HCO_3^-
1	400	201	7.01	13.8	15.9	8.8	16.9	39.3	26.5	67.1
2	1820	1049	7.20	40.6	180.4	54.6	78.8	492.4	145.0	97.6
3	590	321	7.20	21.6	37.0	18.7	32.7	135.3	24.2	73.2
4	1860	1045	7.10	34.0	186.1	57.6	71.8	403.5	252.9	73.2
5	405	553	6.58	20.5	31.5	43.0	65.9	80.5	301.7	30.5
6	314	251	7.20	20.0	23.4	15.0	22.8	73.6	30.7	85.4
7	580	302	6.74	13.4	22.8	20.3	27.4	53.4	128.9	48.8
8	164	248	6.96	11.2	20.4	15.1	26.6	49.6	75.2	61.0
9	204	193	7.05	11.7	16.4	11.3	19.3	39.6	45.7	61.0
10	265	187	6.98	11.5	15.8	10.4	19.5	39.8	28.8	73.2

11	214	186	6.90	13.4	15.8	10.6	18.4	40.1	28.0	73.2
12	312	186	7.13	14.1	16.7	10.2	16.4	40.7	28.5	73.2
13	83	192	6.91	16.0	18.4	10.6	17.5	43.3	29.1	73.2
14	250	233	6.80	10.4	28.3	11.6	18.6	58.6	42.6	73.2
15	440	256	6.98	12.5	18.6	16.9	27.5	47.3	96.5	48.8
16	588	740	6.97	19.4	111.4	58.0	44.5	298.6	166.6	61.0
17	870	472	6.68	23.3	50.5	33.9	40.5	113.3	221.7	12.2
18	1063	604	6.36	27.5	57.8	48.3	49.2	130.6	305.7	12.2
19	316	225	6.48	12.3	20.3	11.1	18.8	33.0	19.4	122.0
20	392	248	7.01	12.6	23.0	15.2	23.8	59.6	65.0	61.0
21	338	199	6.74	14.5	16.7	12.1	21.0	38.6	43.8	67.1
22	210	254	6.64	12.2	22.7	15.3	23.5	56.3	75.4	61.0
23	308	226	6.60	11.9	20.1	14.5	22.4	47.9	60.1	61.0
24	405	246	6.52	13.0	18.1	16.1	23.8	45.2	81.7	61.0
25	742	421	7.80	23.1	63.1	25.6	24.6	179.9	30.1	97.6
26	210	204	7.10	14.4	16.3	12.9	16.4	37.1	36.1	85.4
27	155	199	7.19	12.8	15.1	12.7	17.3	35.9	38.8	79.3
28	694	446	6.92	27.2	49.8	33.6	32.5	123.9	84.0	122.0
29	361	237	8.05	19.2	27.8	11.6	15.0	31.1	17.0	134.2
30	1114	774	7.56	32.7	126.1	46.4	42.3	250.7	125.4	183.0
31	556	390	7.89	24.2	66.4	18.8	18.2	58.4	21.1	207.4
32	285	194	7.74	12.7	20.9	10.7	11.6	32.0	20.7	97.6
33	317	155	7.56	11.8	20.2	10.0	10.8	32.1	21.2	61.0
34	776	479	8.03	13.5	96.7	11.3	18.9	106.6	13.5	231.8
35	298	481	7.00	13.3	100.0	18.8	18.6	121.7	100.2	122.0

Table 2. Correlation coefficient (Pearson's correlation[54]) of different constituents, Bahariya Oasis, Western Desert, Egypt

Variables	EC	TDS	pH	K+	Na+	Mg++	Ca++	Cl-	SO4--	HCO3-
EC	1									
TDS	0.835	1								
pH	0.004	0.010	1							
K+	0.787	0.749	0.000	1						
Na+	0.770	0.900	0.008	0.630	1					
Mg++	0.668	0.871	0.061	0.691	0.630	1				
Ca++	0.685	0.797	0.108	0.643	0.537	0.836	1			
Cl-	0.783	0.880	0.000	0.694	0.877	0.723	0.679	1		
SO4--	0.376	0.492	0.356	0.314	0.236	0.664	0.671	0.248	1	
HCO3-	0.002	0.005	0.511	0.011	0.074	0.026	0.067	0.004	0.244	1

IV. Result and Discussion

Geoelectrical Layers

The gained field curves of (VES) and (TEM) are interpreted in a qualitative and quantitative way. The qualitative interpretation gives initial exploration about variations in the values of apparent resistivity according to the change in depth. Moreover, it is utilized to differentiate the various kinds of curves (David et al., 2018). Comparison between the various kinds of curves can provide more data about the horizontal variations of a layer

or a set of layers (Fig. 2 a, b, and c).

In VES, the change in resistivity values between sequence layers is measured by increasing the inward electrical current (by increasing the distance between current and potential electrodes in geometrical way as in Schlumberger configuration). So, the measured resistivity values points are affected by the integration and accumulation of all the changes in the lithology of rock sequences through which the current passes,especially in arid or semi-arid regions like Egypt, where the surface layers has high earthling (solid or variable soils) and high temperature that affects the electrode connection to the ground. Thus, the deeper the depth is, the less the measurement efficiency is found.

On the contrary, in TDEM method, electromagnetic wave doesn't depend on the integration between layers because (1) it measures the voltage with time at every isolated depth and the resistances of the surface layers are not integrated or affect the measured data from other layers, (2) there are no electrodes that are connected to the earth. So, TDEM can measure the resistivity values that represent the sequences of layers except the surface layer (because of the high attenuation of electromagnetic waves in this surface layer). Therefore, the deeper the depth is, the more accurate the measurements are detected.

The two methods support each other to avoid the weaknesses in each measurement. The VES method is accurate in the shallow layers, and its accuracy decreases with the depth, while the TDEM method is accurate in the deep layers and its accuracy increases with the depth. Therefore, the two methods are used to complete each other to get the best model which represents the change in the resistivity values of successive layers. In addition, both VES and TEM methods are the most useful and important methods in groundwater exploration.

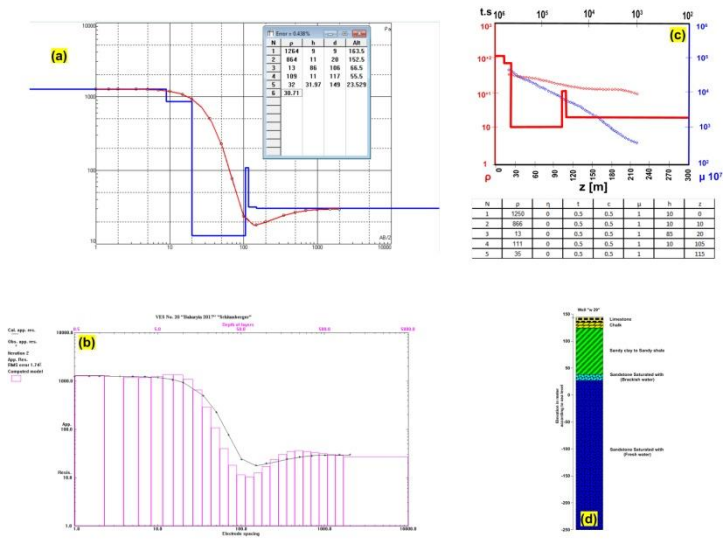

Figure No. 2. Example of the field curves interpretation data in the study area. (a) Interpretation of VES No. 20 by using [41], (b) Interpretation of VES No. 20 by using [42], (c) Interpretation of TEM No. 20 by using [45], (d) Lithology of Well (29) near Station No. 20.

The aim of quantitative interpretation is to explain the geoelectrical parameters, which describe every geoelectrical layer, such as thickness and true resistivity that show the encountered layers' spatial and vertical distribution. The model data is based on the geology of the region, the geological column, resistivity values, and some of the well logging records available in the region. The acquired geoelectrical parameters of the measurements of the two sounding (VES and TEM) illustrate that the geoelectric sequence in the investigated region contains five geoelectrical layers.

Eight geoelectrical cross sections have been drawn in order to identify the geoelectrical layers, specially the water-bearing layers and their circulation in the region under investigation, and to localize the structures that affect the geoelectrical layers. These cross sections intersect the investigated region in NE–SW direction (AA', BB', CC', and DD') and NW–SE direction (EE', FF', GG', and HH'). The following is a short depiction of such geoelectrical successions from the upper layer to the lower layer (Figures 3 a - h,):

- The upper layer consists of Limestone plateau (middle to late Eocene). Its resistivity values range between1235 Ωm at VES 17 and 2355 Ωm at VES 5; and its thickness varies from 2.0m at VES 33 to 80.0m at VES 5. This layer exists around the Bahariya depression in the northern and central parts and disappears within the oasis and in the southern part of the investigated region.
- The second layer consists of Chalk (Early Maastrichtian). Its resistivity values vary from 835 Ωm at VES 17 to 994 Ωm at VES 32; and its thickness ranges between4.0m at VES 19and97.0m at VES 23.Its depth varies from 110.0m at VES 18 to 238.0m at VES 69. This layer appears only around the Bahariya

depression in the southeastern and southwestern flanks parts and disappears within the oasis and in the northern part of the investigated region.

- The third layer consists of Sandy clay to shaley sand. The resistivity values of this layer rangebetween1 Ωm at VES 25and18 Ωm at VES 71; and its thickness varies from 2.0m at VES 26 to 118.0m at VES 71. Its depth ranges between -23.0m at VES 50 and 248.0m at VES 73. The clay and shale layers are acting as capping layers covering the layers of water-bearing (Lithologic log of Well 29, Fig. 2d).
- The fourth layer consists of sandstone saturated with fresh water (Cenomanian Nubian Sandstone). This layer's resistivity values vary from 60 Ωm at VES 76 to 144 Ωm at VES 1; and its thickness ranges between117.0m at VES 9and206.0m at VES 26. Its depth varies from 7.0m at VES 25 to 18.0m at VES 70. This layer is considered the main aquifer of the groundwater in the investigated area.
- The lower layer consists of sandstone saturated with brackish water (Cenomanian Nubian Sandstone). In general, its thickness increases in the direction of the northeast direction. Its resistivity values rangebetween20 Ωm at VES 60and45 Ωm at VES 1; and its depth varies from -180.0m at VES 18 to 131.0m at VES 26.

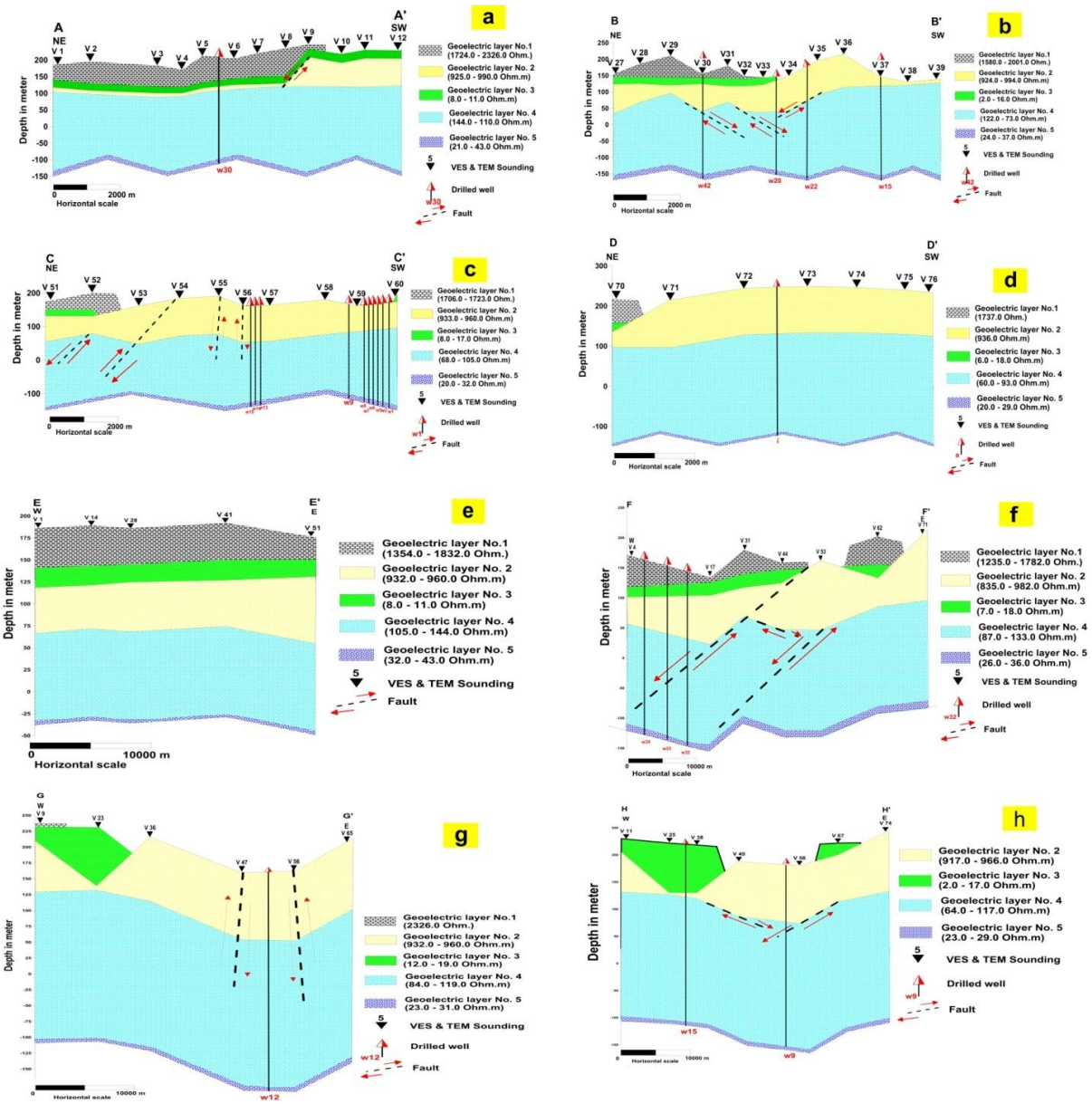

Figure No. 3. a) Geoelectric cross section A-A', b) Geoelectric cross section B-B', c) Geoelectric cross section C-C'', d) Geoelectric cross section D-D', e) Geoelectric cross section E-E', f) Geoelectric cross section F-F', g) Geoelectric cross section G-G', h) Geoelectric cross section H-H'.

Overviewing the five geoelectrical layers, it is noted that the high resistivity values of the first layer are situated in the northeastern part of the study area, while they decrease toward the middle parts (Fig. 4a). The high thickness values of this layer are illustrated in the northeastern parts and in northern flanks of the investigated region, and they decrease toward the middle parts (Fig. 5a), while the high values of the elevation are located in the northeastern and northern parts of the investigated region and decrease toward the middle parts of the investigated region (Fig. 6a).

In the second layer, the high resistivity values are located in the flank parts of the investigated region, while they decrease toward the middle parts (Fig. 4b). The high values of thickness appear in the northwestern parts of the investigated region, the low values of the thickness appear in the northeastern and southwestern parts (Fig. 5b), while the high values of the depth are located in the eastern, southwestern, and northeastern parts of the investigated region, they decrease toward the middle parts until reach its minimum values in the northeastern parts of the investigated region (Fig. 6b).

The high resistivity values of the third layer are located in the central and southern parts of the investigated region, while they reduce toward the outside parts (Fig. 4c). The thickness map of this layer indicates that the high values are found in the central and northeastern and southern to southwestern parts of the investigated region, these values decrease toward the northern, northeastern and northwestern parts of the investigated region (Fig.5c). The great values of the depth are found in the northeastern and they reduce toward the southwestern parts of the investigated region (Fig.6c).

In the fourth layer, the high resistivity values are located in the flank parts of the investigated region, while they reduce toward the central part (Fig. 4d). The high values of thickness appear in the northwestern parts of the investigated region, these values decrease toward the southwestern parts (Fig. 5d), while the high values of the depth are located in the western, southwestern, and northwestern parts of the investigated region and they decrease toward the middle parts. Some low values appear in the northeastern parts of the investigated region (Fig. 6d).

The high resistivity values of the fifth layer are cited in the northern, southwestern and southern parts of the investigated region, while they decrease toward the northeastern parts (Fig. 4e). The depth map of this layer shows that the high values are located in the western, southern, southwestern, and northeastern parts and they decrease toward the northeastern parts of the investigated region (Fig.6e). The ranges of the resistivities and the corresponding thicknesses of the geoelectrical layers are illustrated in table no. 3.

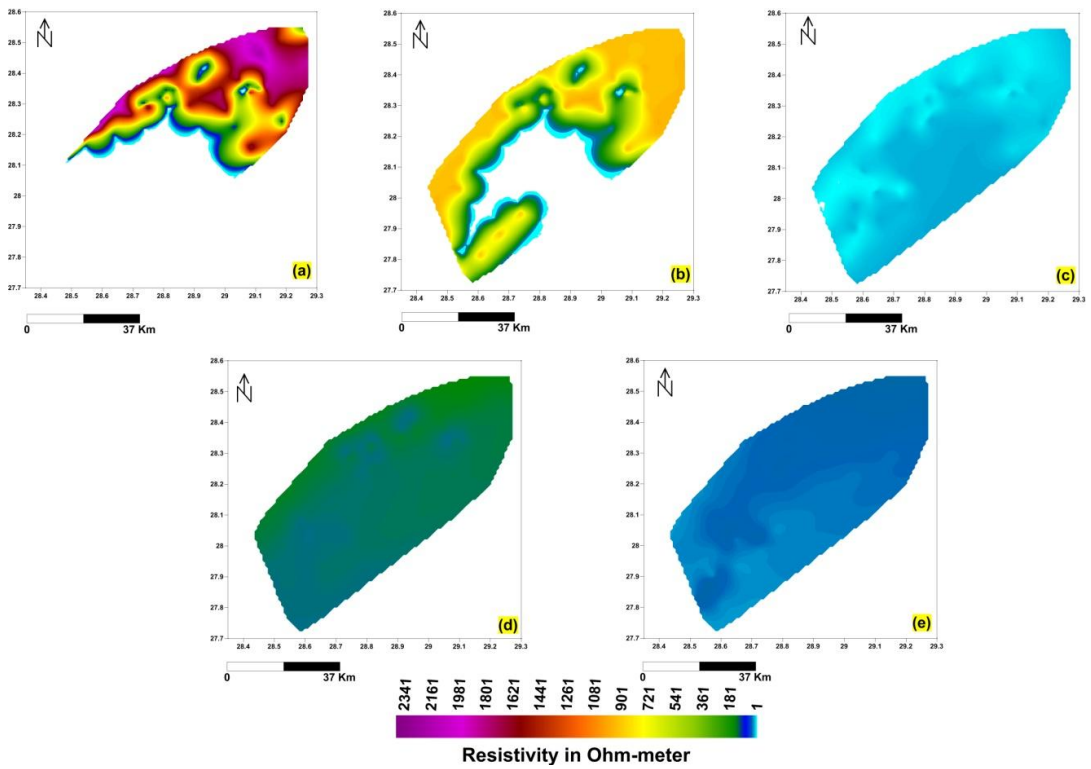

Figure No. 4. The Iso-resistivity contour map of the five geoelectrical layers over the study area, (a) True resistivity contour map of the first geoelectrical layer, (b) True resistivity contour map of the second geoelectrical layer, (c) True resistivity contour map of the third geoelectrical layer, (d) True resistivity contour map of the fourth geoelectrical layer, (e) True resistivity contour map of the fifth geoelectrical layer.

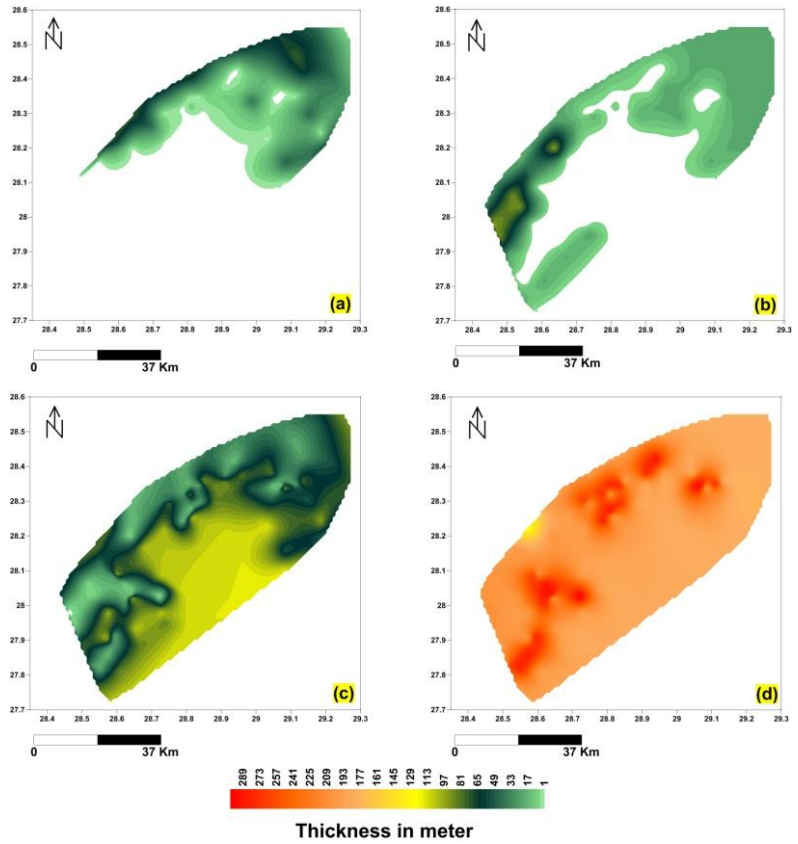

Figure No. 5. The thickness contour map of the five geoelectrical layers over the study area, (a) Thickness contour map of the first geoelectrical layer, (b) Thickness contour map of the second geoelectrical layer, (c) Thickness contour map of the third geoelectrical layer, (d) Thickness contour map of the fourth geoelectrical layer, (e) Thickness contour map of the fifth geoelectrical layer.

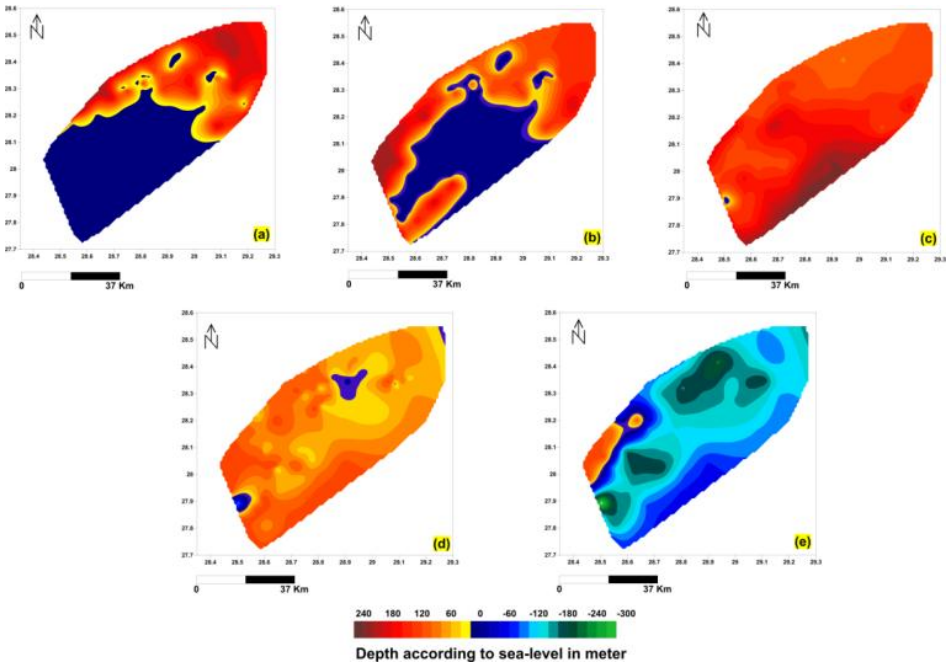

Figure No. 6. The Depth contour map to the upper surfaces of the five geoelectrical layers in the study area, (a) Elevation contour map of the upper surface of the first geoelectrical layer (b) Depth contour map to the upper surface of the second geoelectrical layer (c) Depth contour map to the upper surface of the third geoelectrical layer (d) Depth contour map to the upper surface of the fourth geoelectrical layer (e) Depth contour map to the upper surface of the fifth geoelectrical layer.

Table 3: The ranges of the resistivities and the corresponding thicknesses of the geoelectrical layers

Geoelectrical layers	Resistivity range (Ohm·m)		Thickness range (m)		Lithological description
	Minimum	Maximum	Minimum	Maximum	
First layer (surface)	1235	2355	2	80	Limestone plateau (middle to late Eocene)
Second layer	835	994	4	97	Chalk (Early Maastrichtian)
Third Layer	1	18	2	118	Sandy clay to shaley sand
Fourth layer	60	144	7	18	Sandstone saturated with brackish water (Nubian Sandstone)
Fifth layer	20	45	--	--	Sandstone saturated with brackish water (Nubian Sandstone)

Hydrochemical Characteristics

Durov (1948) diagram

Based on the classification of [54], the majority of the forty two samples are located at the center of the square indicating that there is fresh recent recharge water exhibiting simple dissolution or mixing with no dominant major anion or cation (Fig. 7a).

Schoeller (1977) diagram

Geochemistry of groundwater is discussed by means of its major ions. Plots of collected samples in epm are presented in Figure 7b. The relative tendency of ions shows that Na^+ is the dominant cation in about 74% of the samples while Cl^- is the dominant anion in about 57% of the samples.

Piper (1944) diagram

The subdivisions of diamond-shaped field (Fig. 7c) indicate the hydrochemical facies in forty two water samples. From the [46] tri-linear diagram, it is apparent that the majority of the samples (57%) belong to mixed Ca-Mg-Cl water type (Class 3) demonstrating that such water samples may result from multiple mineral dissolution or mixing of two chemically distinct groundwater bodies. Only 17% of the samples belongs to Ca-Cl water type, where concentrations of sulfate, chloride, magnesium and calcium exceed 50 % of the total meq/l. Figure (7c) is about the plots of the analyzed groundwater samples in the investigated region.

Evaluation for agriculture uses

The Na or alkali hazard is expressed in terms of sodium adsorption ratio (SAR). The SAR values <10 is classified as excellent for irrigation. Values 10-18 are moderate and >18 are hazardous [55]. The relation between SAR and salinity (Fig. 7d) for the analyzed 42 groundwater samples reveals that all the samples have SAR less than 10 can be used for irrigation on almost all soils with no risk of the appearance of harmful exchangeable sodium levels. About 83% of the samples are located in S1C1 and S1C2 fields indicating that this water is suitable for irrigation for many crops. Only 17% of the samples is located in S1C3 field indicating that this water has EC>750 µmohs/cm. So, they can be used to irrigate moderately sensitive crops. Figure (7d) is about the classification of the examined water samples for irrigation, based on [56], in the study area.

Groundwater Potentiality

According to the estimated depth to groundwater in 42 drilled wells (Fig. 1b), the investigated region is divided into three parts of potentiality: high, medium and low. The highest values are found in the middle of the investigated region, surrounded by the middle values, while the low values are found in the rest of the region (Fig. 8a). The groundwater flow direction in the investigated region, measured from collected samples, takes direction of SW-NE. The three major points are located in the northern part of the investigated region indicating high salinity, due to high withdrew and intercalation of clay lenses in these places (Fig. 8b). This shows that the solved salts increase with the direction of groundwater flow from south-west to north-east.

Figure (8a) is about the groundwater potentiality of the investigated region. Figure (8b) is about the direction of groundwater flow according to the salinity contour map in the investigated region.

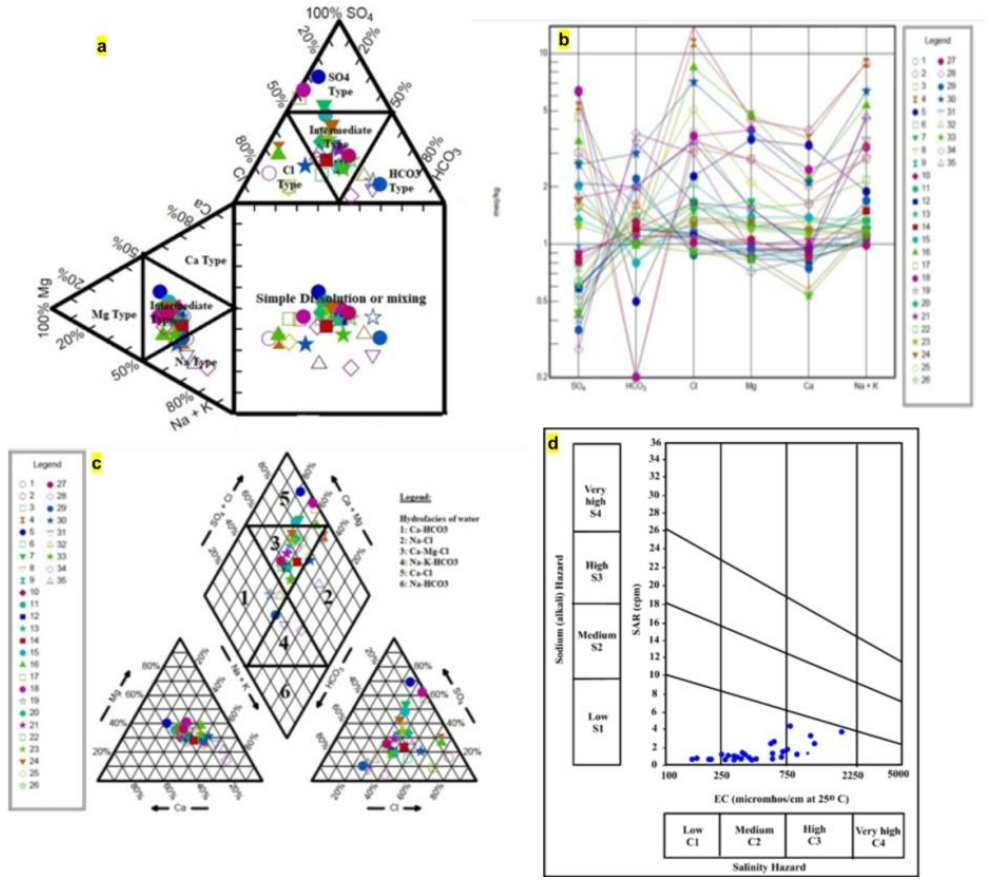

Figure 7. (a) [48] diagram of the groundwater samples, Bahariya Oasis, Western Desert, Egypt. (b) [47] diagram of groundwater samples, Bahariya Oasis, Western Desert, Egypt. (c) Plots of the analyzed groundwater samples, Bahariya Oasis, Western Desert, Egypt, on [46] tri-linear diagram. (d) Classification of the examined water samples for irrigation, based on [56]), Bahariya Oasis, Western Desert, Egypt.

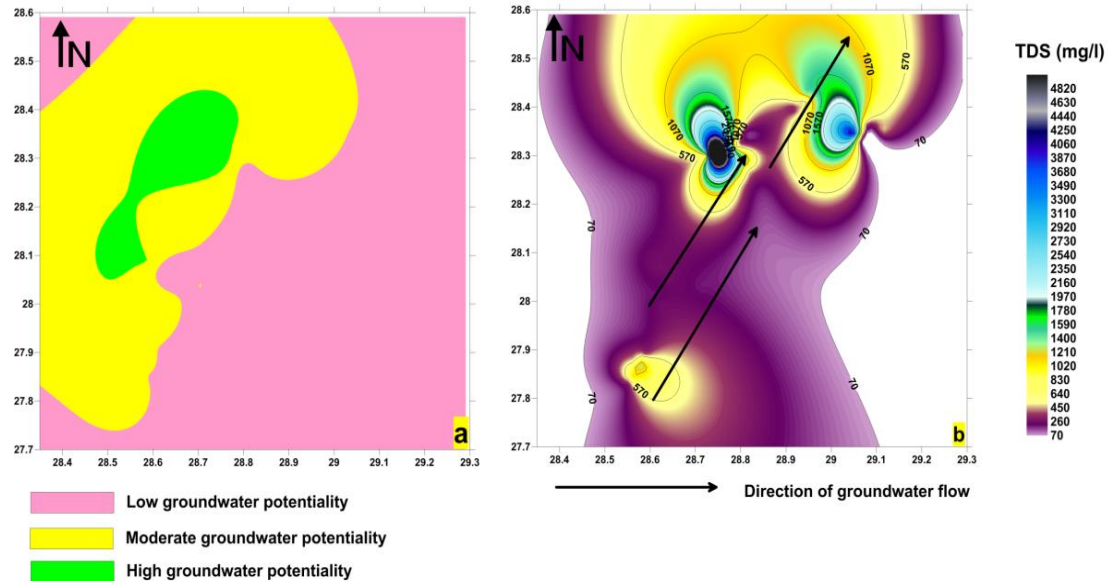

Figure No. 8. a) The groundwater potentiality of the investigated region, b) the direction of groundwater flow according to the salinity contour map in the investigated region.

V. Conclusion

By interpreting the geophysical measured data, it is clear that the subsurface of the investigated region consists of five geoelectrical layers interrupted by many structures. The surface layer consists of central to late

Eocene limestone plateau. Its thickness varies from 2.0m to 80.0m. This layer is located around the Bahariya depression in the north and middle parts only and disappears inside the oasis and in the southern part of the investigated region. The second layer consists of Early Maastrichtian chalk. Its thickness ranges between 4.0m and 97.0m. This layer appears only around the Bahariya depression in the south east and south west flanks parts and disappears within the oasis and in the north part of the investigated region. The third layer consists of Sandy clay to shaley sand. Its thickness varies from 2.0m to 118.0m. This layer is acting as capping layers covering the layers of water bearing. The fourth layer consists of Cenomanian Nubian Sandstone saturated with fresh water. Its thickness ranges between 117.0m and 206.0m. This layer is considered the main groundwater aquifer in the investigated area. The lower layer consists of Cenomanian Nubian Sandstone saturated with brackish water. In general, its thickness increases in the south west direction. Its depth varies from -180.0m to 131.0m.

Most of the 42 groundwater samples, which are collected from the investigated region, shows that new recharge water exists; the matter that reveals that there is humble dissolution or mixture with non-dominant major anion or cation. The corresponding trend of ions illustrates that Na+ is the main cation in about 74% of the samples while Cl- is the main anion in about 57% of the samples. Obviously, (57%) of the samples belongs to mixed Ca-Mg-Cl water type, indicating that these water samples may possibly arise from various mineral dissolution or the mixing of two chemically separate groundwater layers. (17%) of the samples refers to Ca-Cl water type, in which the concentrations of S, Cl, Mg and Ca are over 50 % of the whole meq/l.

It is possible for the entire samples that have > 10 SAR to be used for irrigation on just about the entire soils with no risk of the presence of dangerous levels of exchangeable sodium. About (83%) of the samples has EC<750 µmohs/cm, indicating that this water is appropriate for irrigating many normal crops, whereas (17%) has EC>750 µmohs/cm, indicating that this water is appropriate for irrigating reasonably sensitive crops.

References

[1]. **Plyusnina EE, Sallam ES, Ruban DA (2016)** Geological heritage of the Bahariya and Farafra oases, the central Western Desert of Egypt, Journal of African Earth Sciences, January 2016, doi: /j.jafrearsci, vol. 4, p. 151-159.

[2]. **Abd El-Gawad EA, Mousa DA, Lotfy MA, El-Shorbagy AI (2017)** Origin of Bahariya oil in Salam oil field, Western Desert-Egypt, Egyptian Journal of Petroleum, https://doi.org/10.1016/j.ejpe.2017.09.003.

[3]. **El-Akkad S and Issawi B (1963)** Geology and iron ore deposits of the Bahariya Oasis, Geological Survey and Mineral Research Department, Egypt, Paper 18p. 301.

[4]. **Mohamed I Abdel-Fattah, John D Pigott, Zakaria M Abd-Allah (2017)** Integrative 1D-2D Basin Modeling of the Cretaceous BeniSuef basin, Western Desert, Egypt., Research article, Journal of Petroleum Science and Engineering, Volume 153, May 2017,P. 297-313.

[5]. **Mohamed Yousif, Hassan S Sabet, Saad Y Ghoubachi, Ameer Aziz (2018)** Utilizing the geological data and remote sensing applications for investigation of groundwater occurrences, West El Minia, Western Desert of Egypt, NRIAG Journal of Astronomy and Geophysics, Volume 7, Issue 2, December 2018, P. 318-333.

[6]. **El Hossary M (2013)** Ensuring sustainable development via groundwater management (case study: El-Bahariya Oasis); Journal of American Sciences. 9 (6), p. 6–13.

[7]. **Hobbs, W.H. (1904)** Lineaments of the Atlantic Border Region. Geological Society. American Bulletin, 15, 483-506.

[8]. **Bonn, F., & Rochon, G. (1992)** Précis de télédétection volume 1: Principes et méthodes. Sainte- Foy: Presse de l'université du Québec/AUPELF, 485 p.

[9]. **Kouamé, K.F. (1999)** Hydrogéologie des régions de montagne: Apports des données de télédétection et des méthodes statistique et fractale à l'élaboration d'un système d'information hydrogéologique à référence spatiale des aquifères discontinus du secteur Man-Danané. (Ouest de la Cote d'Ivoire). Thèse de Doctorat 3è cycle, Université de Cocody.

[10]. **Gadallah M M, Samir A, Ashraf Ghoneimi, Mohammad Nabih (2004)** Seismic and well logging analysis of Bahariya Formation in Aghar oil field, northern Western Desert, Egypt, September 2004, Conference: The Tenth Formation Evaluation Symposium of Japan.

[11]. **Jordan, P., Arnscheidt, J., McGrogan, H., McCormick, S. (2005**) High-resolution phosphorus transfers at the catchment scale: the hidden importance of non-storm transfers. Hydrology and Earth Systems Sciences, 9(6):685-691

[12]. **Rashad Sawires (2011)** Potentiality and suitability of groundwater in the northern part of El-Baharyia Oasis, Western Desert, Egypt. April 2011, The 3rdConference for Young Scientists, Assiut University, Egypt, p. 64-70.

[13]. **Azab AA (2014)** Agnes high, Western Desert, Egypt: A structural study in view of potential data modeling, Egyptian Journal of Petroleum, https://doi.org/10.1016/j.ejpe.2014.05.010 , Volume 23, Issue 2, June 2014, P. 229-245.

[14]. **Masoud M H and El Osta M. M. (2016)** Evaluation of groundwater vulnerability in El-Bahariya Oasis, Western Desert, Egypt, using modelling and GIS techniques: A case study, Journal of Earth System Science, August 2016, Volume 125, Issue 6, pp 1139–1155.

[15]. **Al-Garni MA, Hassanein HI, and Gobashy MM (2005)** Ground magnetic survey and Schlumberger sounding for identifying the subsurface factors controlling the groundwater flow along Wadi Lusab, Makkah Al-Mukarramah, Saudi Arabia. Journal of Applied Geophysics, National research institute, Egypt, 4, 59–74.

[16]. **Abdel Zaher M, Saibi H, El Nouby M, Ghamry E, and Ehara S (2011)** A preliminary regional geothermal assessment of the Gulf of Suez, Egypt. Journal of African Earth Science, 60,117–132.

[17]. **Rabeh T, Miranda JMM, Carvalho J, and Bocin A (2011)** Interpretation case study of the Sahl El Qaa area, southern Sinai Peninsula, Egypt. Journal of Geophysical Prospecting, vol. 57, p. 447–459.

[18]. **Sameh Saadi, Gilles Boulet, Malik Bahir, Aurore Brut, Emilie Delogu, Pascal Fanise, Bernard Mougenot, Vincent Simonneaux, Zohra Lili Chabaâne, Zohra Chabaane (2011)** Assessment of actual evapotranspiration over a semiarid heterogeneous land surface by means of coupled low-resolution remote sensing data with an energy balance model : comparison to extra-large aperture scintillometer measurements. Hydrology and Earth System Sciences, European Geosciences Union, 2018, 22 (4), pp., 2187 – 2209, 10.5194/hess-22-2187-2018, ird-01762227.

[19]. **Zohdy AAR (1989)** A new method for the automatic interpretation of Schlumberger and Wenner sounding curves. Journal of Geophysics, vol. 54, p. 245– 253.

[20]. **Zohdy MA, K Gu K, and Loh NK (1989)** Necessary and sufficient conditions of quadratic stability of uncertain linear systems., Conference of Tampa, FL, USA, USA, 13-15 Dec. 1989, INSPEC Accession Number: 3684918, DOI: 10.1109/CDC.1989.70157, Publisher: IEEE, p. 128.

[21]. **Abdel Zaher M, Sultan AS, El-Said AA, and Ehara S (2008)** Geophysical Study of the Sedimentary Cover in Darb El-Arbeen, South Western Desert, Egypt. Memoirs of the Faculty of Engineering, Kyushu University, vol. 68, p. 83–92.

[22]. **Massoud, U, Santos F, Khalil MA, Taha A, and Abbas AM (2010)** Estimation of aquifer hydraulic parameters from surface geophysical measurements: a case study of the Upper Cretaceous aquifer, central Sinai, Egypt. Hydrogeology Journal, Vol. 18, p. 699–710.

[23]. **El Kashouty M, Abdel Aziz A, Soliman M, and Mesbah M (2012)** Hydrogeophysical investigation of groundwater potential in the El- Bawiti, Northern Bahariya Oasis, Western Desert, Egypt. Arabian Journal of Geosciences, 5, 953–970.

[24]. **Hewaidy AA, El-Motaal EA, Sultan AS, Ramdan TM, El khafif AA, and Soliman SA (2015)** Groundwater exploration using resistivity and magnetic data at the northwestern part of the Gulf of Suez, Egypt. Egyptian Journal of Petroleum, 24, p. 255–263.

[25]. **El Shazly MM, El-Ramly IM, Sallouma MK. and Abd El-Baki AA (1993)** Groundwater quality in relation to its impact on the corrosion of pipes and the pumping equipment of the water wells in Al Bahariya Oasis, Western Desert, Egypt., Egyptian Journal of Geology, V.37, No.2, pp. 21-38.

[26]. **Sehim AA, (1993)** Cretaceous tectonics in Egypt, Egyptian Journal of Geology, 1993, vol. 371, p. 335- 372.

[27]. **Moustafa AR, Saudi A, Moubasher A, Mohamed I. Molokhia H and Schwartz B (2003)** Structural setting and tectonic evolution of the Bahariya Depression, Western Desert, Egypt. Geo Arabia, Gulf Petrolink, Bahrain, Vol. 8, No.1, p. 91-124.

[28]. **Abd El-Motaal E and Kusky TM (2003)** Tectonic evolution of the Intra-plate S-Shaped Syrian Arc Fold-Thrust Belt of the Middle East Region in the Context of Plate Tectonic., The third International Conference on Geology of Afric Vol. (2), P-P. 139-157, Assiut., Egypt.

[29]. **Said, R (1962)** The Geology of Egypt, Elsevier, Amsterdam, p. 377.

[30]. **Hemida I H (1970)** Local Hydrogeological and hydrochemical characteristics of the artesian aquifer in the Western Desert, Egypt". Symposium of applied and scientific researches of groundwater in Egypt, vol. I. p. 8-17. (in Arabic)

[31]. **Amer HI (1973)** Geological and mineralogical studies on the Bahariya Oasis and their iron ore deposits, Western Desert, Egypt. PhD thesis, Faculty of Science, Cairo University, Egypt, p. 121.

[32]. **Diab M.S, Zeidan S and Himida IH (1978)** Recent study of the hydrogeology of Bahariya Oasis, Western Desert, Egypt. 10th Arab Petroleum Congress, Tripoli, Libya, Paper No. 140 (B-3), p. 14.

[33]. **El Bassyony AA (1978)** Structure of the Northwestern plateau of the Bahariya Oasis, Western Desert, Egypt. Geologe En Mijnbouw 57(1), p. 77–86.

[34]. **Embabi NS, El Kayali MA (1979)** A morphotectonic map of the Bahariya depression. Ann. Geology Survey of Egypt, vol. VIX, p. 179–183.

[35]. **El Mansy IM, Ragab MA, and El Gendy NH (1989)** Studies on petrologic and petrophysical properties of some Cambrian and Lower Cretaceous core samples from Bahariya Oasis, Western Desert, Egypt. Faculty of Science Journal, Menoufia University Vol. III, p. 79-90.

[36]. **Abdel Ati, AA, (1995)** Groundwater conditions in El-Bahariya Oasis and future development. M.Sc. Thesis, Fac. Sci., Cairo Univ., 172 p.

[37]. **Abdel Ati, AA (2002)** Hydrogeological studies on the Nubian Sandstone Aquifer in Bahariya and Farafra depressions, Western Desert, Egypt. Ph.D. Thesis, Fac. Sci., Ain Shams Univ., 164 p.

[38]. **Abdel Latif RK (2006)** Study of groundwater resources management in Bahariya Oasis, Western Desert, Egypt.PhD thesis, Faculty of Science, Alexandria University, Egypt.

[39]. **Syscal pro instrument.** all-in-one multi-node resistivity and induce polarization sounding and profiling system for environmental and engineering geophysical studies. http://www.iris-instruments.com/syscal-pro.html

[40]. **Iboukoun Christian Alle, Marc Descloitres, Jean-Michel Vouillamoz, NicaiseYalo, Akonfa Consolas Adihou (2018)** Why 1D electrical resistivity techniques can result in inaccurate sitting of boreholes in hard rock aquifers and why electrical resistivity tomography must be preferred: the example of Benin, West Africa**.** Journal of African Earth Sciences, Volume 139, March 2018, P. 341-353.

[41]. **RES1D program (GEOTOMO) (2001)** IP inversion using the least-squares method. www.geoelectrical.com, RES1D ver. 1.0for Windows 95/98/Me/2000/NT, 1-D Resistivity, IP & SIPInversion and forward modeling, Wenner and Schlumberger arrays, M.H.Loke, March 2001, manual, https://www.geotomosoft.com/downloads.php.

[42]. **IPI2Win Software (2003)** Resistivity Sounding Interpretation, Moscow State Univ. Version 3.0.1.a. http://geophys.geol.msu.ru/ipi2win.htm.

[43]. **AIE-2 TDEM** http://zond-geo.com/english/services/equipment/aie-2-instruments/

[44]. **Mahad S Baawain, Ahmed M Al-Futaisi, A Ebrahimi, Hamid Omidvarborna (2018)** Characterizing leachate contamination in a landfill site using Time Domain Electromagnetic (TDEM) imaging, Journal of Applied Geophysics, Volume 151, April 2018, Pages 73-81.

[45]. **ZOND TEM1D Program** http://zond-geo.com/english/zond-software/electromagnetic-sounding/zondtem1d/

[46]. **Piper AM (1944)** A graphical procedure in the geochemical interpretation of water analysis. Eos Trans. Am. Geophys.Union vol. 25, p. 914-923.

[47]. **Schoeller H (1977)** Geochemistry of Groundwater. In: Brown, R.H., Konoplyantsev, A.A., Ineson, J. and Kovalevsky, V.S., Eds., Groundwater Studies: An International Guide for Research and Practice, UNESCO, Paris, p. 1-18.

[48]. **Durov, S.A. (1948)** Natural Waters and Graphic Representation of Their Composition. Doklady Akademii Nauk SSSR, 59, 87-90.

[49]. **Rockware Aq.QA Software** Water Data Analysis tab to perform water dataquality. https://www.rockware.com/product_page/aqqa-data-analyses/

[50]. **Rabeh et al. (2018)** Imen Rabeh, Khaoula Telahigue, Safa Bejaoui, Tarek Hajji, Lassaad Chouba, M'hamed EL Cafsi &Nejla Soudani., Effects of mercury graded doses on redox status, metallothionein levels and genotoxicity in the intestine of sea cucumber Holothuria forskali, , Journal of Chemistry and Ecology, Volume 35, 2019 - Issue 3, Published Online: 15 Nov 2018.

[51]. **Srivastava KS and Ramanathan LA (2008)** Geochemical Assessment of Groundwater Quality in Vicinity of Bhalswa Landfill.Delhi; India by Using Graphical and Multivariable Statistical Methods. Environmental., Geology, vol. 53, p. 1509-1528. http://dx.doi.org/10.1007/s00254-007-0762-2.

[52]. **Naseem Shahid, Hamza Salma, and Erum Bashir (2010)** Groundwater Geochemistry of Winder Agricultural Farms, Balochistan, Pakistan and Assessment for Irrigation Water Quality. EWRA, eurupean water, Vol. 31, PP. 21-32, 2010, EW publications.
[53]. **David Nakamura Leite, Cassiano Antonio Bortolozo, Jorge Luís Porsani, Marco Antonio Couto, Marcelo César Stangari, (2018)** Geoelectrical characterization with 1D VES/TDEM joint inversion in Urupês-SP region, Paraná Basin: Applications to hydrogeology, Journal of Applied Geophysics, Volume 151, April 2018, Pages 205-220.
[54]. **Lloyd JW and Heathcoat JA (1985)** Natural Inorganic Chemistry in Relation to Groundwater. Clarendon Press, Oxford. 455 p.
[55]. **Fipps, Guy (1996)** Irrigation Water Quality Standards and Salinity Management, Texas A&M University. P. 20.
[56]. **U.S. Salinity Laboratory Staff, (1954)** Diagnosis and improvement of salinity andalkaline soil. USDA Hand Book no. 60, Washington.

Alhussein Adham. "Employing the geophysical and hydrological data for the evaluation of the groundwater occurrences in Baharyia Oasis, Egypt."*IOSR Journal of Applied Geology and Geophysics (IOSR-JAGG),* 8(1), (2020): pp. 23-35.